

Change detection of groundwater level and quality in coastal aquifers of Malabar region in Kerala

Abstract

A study was conducted to assess the changes in groundwater level and quality for the period 2005-2020 in the coastal aquifer of the Vatakara-Koyilandy stretch in the Kozhikode district of Kerala. Hydrogeochemical analysis of groundwater quality parameters, irrigation water quality analysis and preparation of spatial variability of groundwater level and salinity were used for the study. The Piper diagram was used to track the change in the hydrochemical parameters of groundwater sources in 2005 and 2020 and identify changes in the chemical facies of the groundwater. The Gibbs diagram was used to identify the source of the dissolved ions present in the groundwater in both years. The United States Salinity Laboratory diagram was used to assess the groundwater's suitability for irrigation. The spatial variation of water table elevation and salinity were compared using the ordinary kriging method of interpolation. An increase in seawater intrusion into the wells and a reduction in irrigation water quality was indicated by the change in the Hydrochemical facies, and the shifting of more groundwater samples in the evaporation dominance zone in the Gibbs plot. The spatial variability of groundwater level indicates a reduction in premonsoon in both years. On the North coast, a 4% increase in the area under groundwater level < 2m. the reduction in the groundwater table on the coast increases the chance of seawater intrusion and thereby increased salinity. Even though the study area receives heavy rainfall during monsoon and recharging of the coastal aquifer, seawater intrusion progressed landward from 2005 to 2020 during the premonsoon and affected the groundwater level and quality over this period.

Keywords: Aquifer characterisation, Hydrochemical analysis, Spatial prediction, Groundwater, Seawater intrusion

1. INTRODUCTION

Groundwater is a dynamic and replenishing natural resource. There has been an increase in groundwater extraction as a result of the sharp rise in demand for agricultural, industrial, and home uses. Both the quantity and quality of groundwater are declining in most of India. The issue appears to be more severe when the land meets the sea, especially coastal aquifers. Unsustainable groundwater extraction brought on by growing urbanisation contributes to ecological and environmental problems such as coastal erosion, ground subsidence, seawater intrusion, and coastal floods. (Michalopoulos & Dimitriou, 2018). Studies of the spatial distribution of groundwater quality and level over time can help identify vulnerable locations and shed light on how the problem's geographic scope varies over time.

Groundwater statistical analysis, spatiotemporal variability of the issue, and the relevance of trends in data with seasonality are all very helpful in identifying changes and predicting projections for the future. Hydrochemical facies, mechanisms

22 governing groundwater chemistry, saltwater intrusion status in agriculture,
23 development of a water quality index, and major cation and anion interpolation are a
24 few frequent analyses to look into the geochemical process, source of contamination,
25 and irrigation suitability of groundwater. Using the Gibbs diagram, it is common
26 practice to thoroughly analyse geochemical processes and the mechanisms that
27 control them.

28 The spatial variability map of groundwater depth and quality indicators for the
29 National Capital Territory of Delhi, India, was created by Dash et al., (2010). The
30 geographic variability of groundwater depth and quality was investigated using
31 ordinary kriging. The semivariogram parameters were found to fit well in both the
32 exponential and spherical models for water depth and water quality parameters.
33 Based on data from 97 wells monitored over 7 years, Arslan, (2012) conducted
34 spatial and temporal assessments of groundwater salinity in Bufra Palin, Turkey.
35 ArcGIS Geostatistical Analyst used an explanatory data analysis, semivariogram
36 model selection, cross-validation, and the generation of a groundwater salinity
37 distribution pattern. Ordinary Kriging (OK) was used to investigate groundwater
38 salinity variations over time, whereas Indicator Kriging (IK) was utilised to investigate
39 groundwater salinity about pollution threshold values. With a total of 123 water
40 samples, including 105 unconfined groundwater samples, Zhang et al., (2012)
41 investigated the hydrogeochemical characteristics of groundwater in the Delingha
42 area, northwest China. Hydrochemical types in groundwater were studied using the
43 Piper diagram. Gibbs diagram was used to identify hydrogeochemical evolution,
44 which involves precipitation, rock weathering, and evaporation–crystallization
45 processes. The findings revealed that groundwater hydrochemistry had a distinct
46 zoning pattern in this location.

47 To determine the suitability of groundwater for irrigation and drinking, a
48 hydrogeochemical analysis was conducted in and around the Veeranam tank region
49 by Sathiamoorthy & Ganesan, (2018). The Sodium Percentage, Wilcox Diagram,
50 Alkalinity and Salinity Hazard, Magnesium Hazard, and Residual Sodium Carbonate
51 are used to determine the irrigation water quality. They categorized the samples
52 according to the Wilcox and USSL classifications. Lanjwani et al., (2021) used ArcGIS
53 10.5 to map the spatial variation of groundwater quality in Larkana of Sindh, Pakistan
54 using the IDW method. The water quality index (WQI) was created to categorise
55 suitability for drinking based on various parameters.

56 The objective of this study is to assess the changes in groundwater level and
57 quality for the period 2005-2020 by analysing the pre- and post-monsoon trends,
58 preparing the spatial prediction maps, studying the hydrochemical types,
59 hydrogeochemical evolution, and preparing the irrigation water quality index.

60 **2. MATERIALS AND METHODS**

61 **2.1 Study Area**

62 The study area is situated in the north part of Kerala's Kozhikode coast, the
63 central part of the Malabar coast in India. The study area lies between 75° 03'-75°
64 02' East longitudes and 11° 02'-11° 05' North latitudes with a total area of 270 km²
65 (Fig.1). the climate of this study area is tropical and humid with an average annual
66 rainfall of 2700 mm out of this, 60 % is received during the South-west monsoon and
67 25% is received during the North-East monsoon. The rest of the rainfall occurs in

68 other seasons. December-January to March-April are the dry months. The study area
69 has a humid tropical climate with an average temperature of 27° C.

70 **2.2 Geology**

71 The various geological formations in the study area comprise alluvium deposits
72 that are underlain by laterite and sedimentary rocks, mostly charnockites with mafic
73 granulite enclaves. Laterites occur as capping of these rocks which formed as the as
74 a residue of tropical weathering of crystalline rocks. Groundwater in weathered
75 crystallines is present under unconfined conditions and semi-confined in deep
76 crystalline formations. Groundwater table depth ranges from 0.73 m to 16.11 m below
77 ground level(CGWB, 2013). The well logs of representative wells suggest aquifer
78 consists of three layers namely; the top unconfined layer, an aquitard and a semi-
79 confined aquifer at the bottom.

80 **2.3 Geomorphology and soil types**

81 The geomorphology of Kozhikode district can be categorised as a coastal
82 region in the west, midland in the central part and highland in the east. The study
83 area was delineated with elevation within 10 m from MSL extending over the coastal
84 region and midlands. The soil types in the region are coastal alluvial soil in coastal
85 plain and in low-lying areas, riverine alluvial soil along riverbanks, red loam soil and
86 brown hydromorphic soil (KSPCB, 2019; Nair, 1987; Nazimuddin, 1993). The alluvium
87 deposits are underlain by laterite and sedimentary rocks, mostly charnockites with
88 mafic granulite enclaves. The coastal zone is covered by excessively drained to
89 moderately drained sandy deposits, and the alluvium deposits are covered by
90 excessively drained to moderately drained sandy deposits (CGWB, 2013; KSPCB,
91 2019; Salaj et al., 2018). The soil conditions are ideal for growing coconuts, spices,
92 and plantation crops, and are average for other crops. Coconut, spices, paddy and
93 plantation crops are the most important crops cultivated in the study area.

94 **2.4 Frequency analysis of rainfall**

95 The present study uses 100-year continuous rainfall data acquired from IMD
96 gridded data. The Weibull Plotting position formula was applied to the rainfall data to
97 compute the probability of rainfall's exceedance of rainfall. The probability of
98 exceedance of rainfall is

$$T = \frac{m}{(N + 1)}$$

99 given by,

100 where m is the order or rank and N is the total number of events

101 **2.5 Log-normal distribution**

102 The maximum rainfall for a particular return period was calculated using the
103 log-normal distribution which is a probability distribution of a random variable whose
104 logarithm is normally distributed. The following equation was used to compute the
105 maximum rainfall for a particular return period

106

Where X_{av} is the mean value, k is the frequency factor and

$$XT = X_{av} + k\sigma$$

$$\sigma = \left[\frac{\sum (X_i - X_{avg})^2}{N - 1} \right]^{1/2}$$

107 σ is the standard deviation and N is the sample size and the value of k is
108 determined considering the coefficient of skewness as zero.

109 2.6 Hydrogeochemical Analysis

110 Data on the concentration of major ions such as HCO_3^- , Cl^- , Ca^{2+} , Mg^{2+} , Na^+ ,
111 etc K^+ were used for hydrochemical analysis using the Piper diagram. The trilinear
112 Piper diagram proposed by (Piper, 1944), was applied to plot the concentration of
113 major cations and anions to determine changes that occurred on the chemical facies
114 of the groundwater in 2005 and 2020 to identify the evolution of hydrochemical
115 parameters of groundwater sources in this period. The Trilinear Piper diagram was
116 constructed with the help of Geochemical analyst software version 2015.1.14.

117 Gibb's diagrams are a tool for understanding groundwater chemistry's various
118 mechanisms and processes (Gibbs, 1970). The source of the dissolved ions in the
119 groundwater can be understood by the Gibbs diagram which is a plot of $(\text{Na}^+)/(\text{Na}^+ +$
120 $\text{Ca}^{2+})$ vs TDS and $\text{Cl}^-/(\text{Cl}^- + \text{HCO}_3^-)$ vs TDS. Gibbs diagram was prepared for the
121 years 2005 and 2020 with the help of GRAPHER software.

122 2.7 Irrigation Water Quality

123 The United States Salinity Laboratory diagram (USSL diagram) for the suitability of
124 water for agricultural uses was used to determine the suitability of groundwater for
125 irrigation. Sodium percentage determines the ratio of sodium to the total cations viz.,
126 sodium, potassium, calcium and magnesium. The diagram for the years 2005 and
127 2020 were prepared using GRAPHER software.

128 SAR was prepared using the following formulae

$$129 \text{ SAR} = \frac{\text{Na}^+}{\frac{\sqrt{\text{Ca}^{2+} + \text{Mg}^{2+}}}{2}}$$

130 Where, the ionic concentrations are expressed in meq/l.

131 2.8 Spatial Variation of Groundwater Level and Salinity

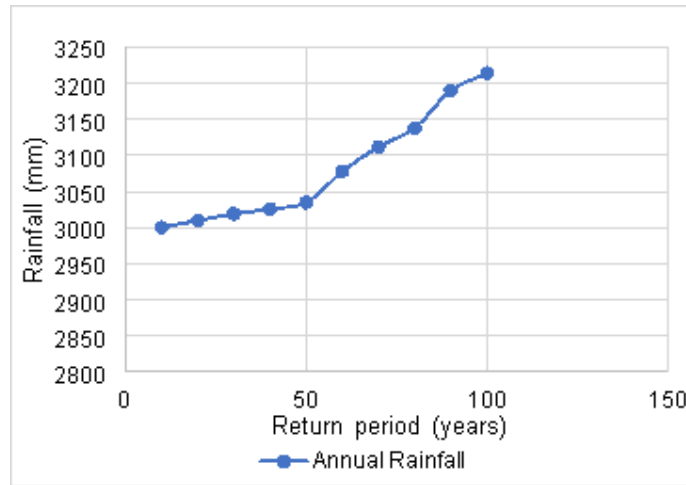
132 Geostatistical tools were used to describe the spatial variability of groundwater levels
133 and salinity. Ordinary kriging was used to plot the spatial variability map of
134 groundwater salinity and levels (Isaaks & Srivastava, 1989).

135 3. RESULTS AND DISCUSSION

136 3.1 Rainfall Extreme Probability Analysis

137 The method of rainfall extreme probability analysis was used to examine the
138 maximum annual rainfall. The maximum rainfall depths for various return periods are
139 presented in Fig. 1, those were calculated using the Plotting Position Formula
140 (Sabarish et al., 2017) and the variation of annual rainfall is presented in Fig. 2.
141 According to the analysis of the annual rainfall for various return periods, the annual

142 rainfall between the 50- and 100-year return periods differs by 180 mm. For the 10-,
 143 30-, and 100-year return periods, the annual rainfall values are 3000, 3019, and 3214
 144 mm, respectively.

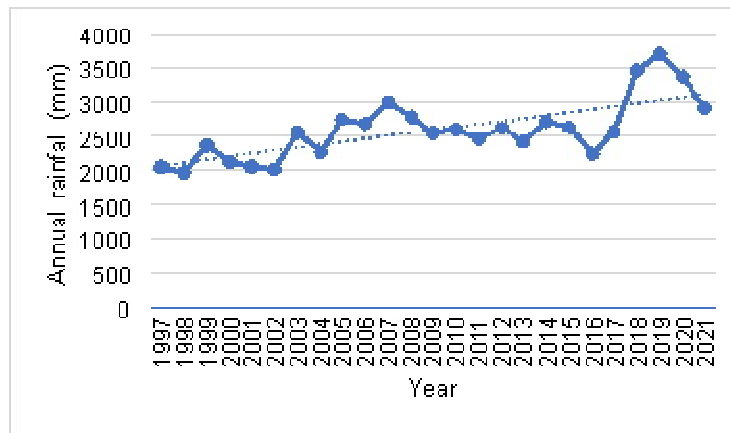


145

146

Fig. 1 Maximum annual rainfall Vs Return Period

147 50% of the land in Kerala is hilly or ghat dominated and the west is bounded by
 148 the Arabian sea. The results showed that the district is highly vulnerable to heavy
 149 rainfall. The heavy rain during the monsoon, or a low-pressure area, and interaction
 150 from wind from the sea. Heavy rainfall in the fragile ecosystem with laterite soil will
 151 cause damage to the ecosystem.
 152



153

154

Fig. 2 Variation of annual rainfall during the 15 years

155 **3.2 Statistical summary of groundwater level and salinity**

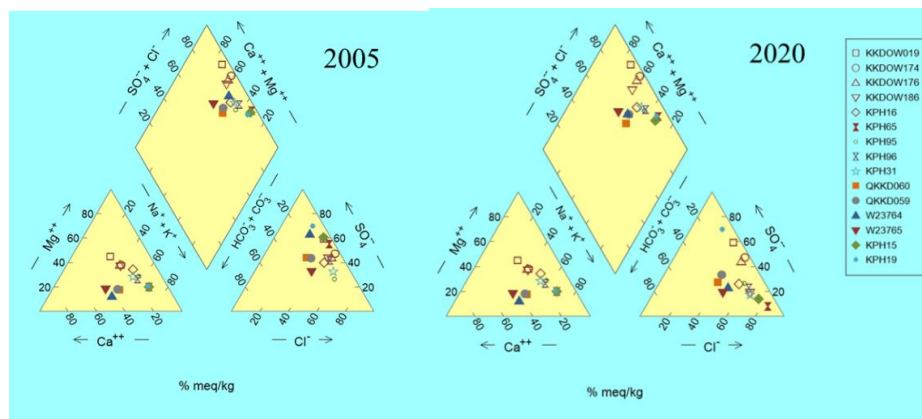
156 The statistical summary of groundwater level and salinity were given in Table 1. The
 157 minimum groundwater elevation in the study area was -0.23 m in 2005 and reduced
 158 to -0.61 m in 2020. The corresponding EC values were 0.87 dS/m and 0.96 dS/m.
 159 The mean values of EC were 1.96 dS/m in 2005 and 2.61 dS/m in 2020. This
 160 indicates a direct relationship between groundwater salinity with the reduced
 161 groundwater level in the area. The mean value of pH in both years resulted in 7.9.

	GW level	TDS	EC	pH
2005				
Minimum	-0.23	0.22	0.67	7.6
Maximum	6.35	2.83	3.18	8.6
Mean	3.73	1.13	1.96	7.9
STDV	1.09	0.48	0.52	0.6
2020				
Minimum	-0.61	0.49	0.96	7.5
Maximum	5.58	2.95	3.96	8.7
Mean	3.01	1.87	2.61	7.9
STDV	1.22	0.47	0.51	0.5
GW level: Groundwater level (m), TDS: Total Dissolved Solids (kg/m ³), EC: Electrical conductivity (dS/m)				

162 3.3 Hydrogeochemical analysis

163 3.3.1 Piper diagram

164 The Hill–Piper trilinear diagram (Piper, 1944), consists of triangle and
 165 diamond-shaped fields with subdivisions representing the various water types and
 166 hydrochemical facies that existed in the aquifer (Ali & Ali, 2018). These
 167 hydrogeochemical facies present in the aquifer for the years 2005 and 2020 shed
 168 light on the changes that occurred in the geochemical process influencing the
 169 groundwater quality in the aquifer (Fig.3).



170

171

Fig. 3 Hydrochemical facies in 2005 and 2020

172

173

174

175

176

177

178

179

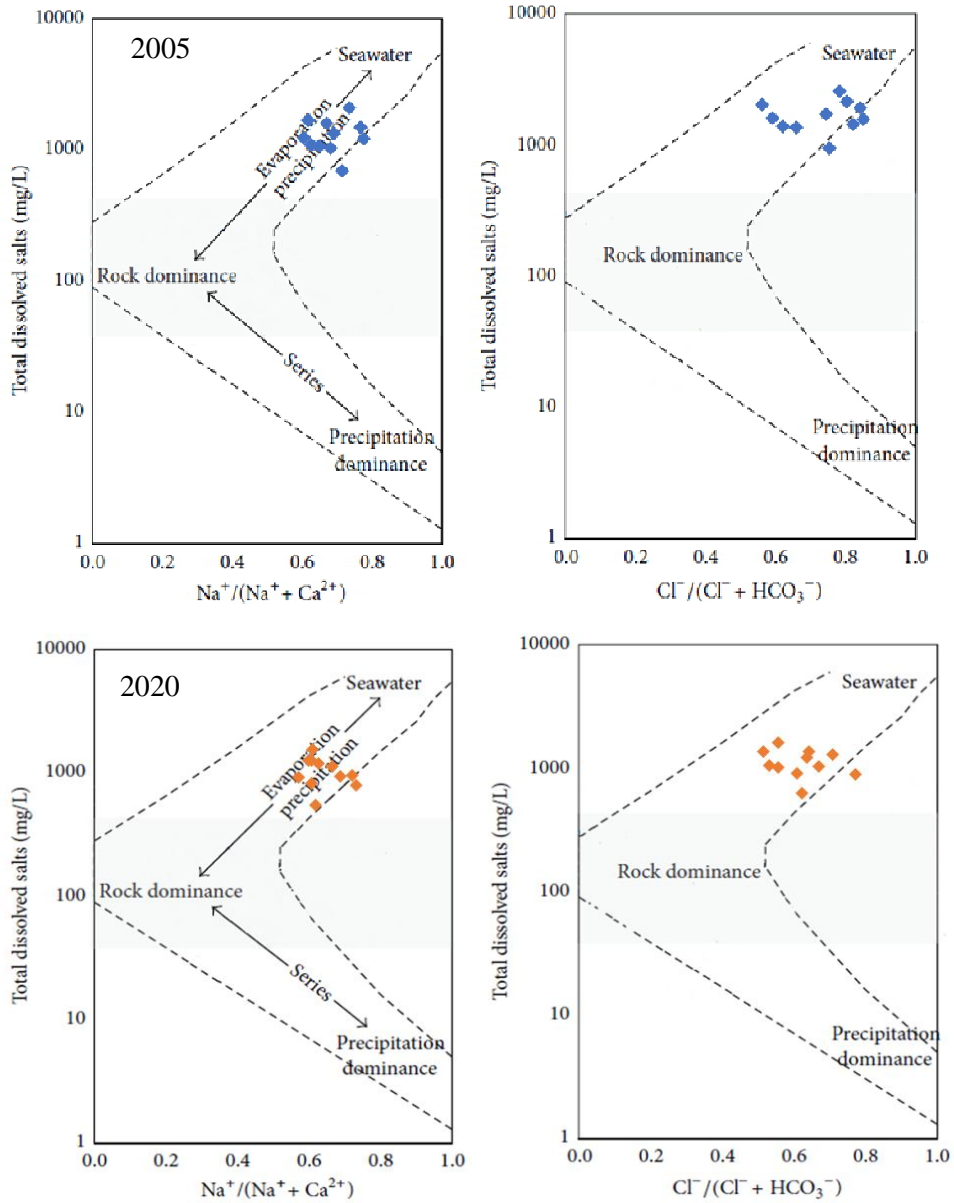
180

181

From the cationic triangular field of the Piper diagram in 2005, 45% of the samples fall into the no dominant type, conversely, 55% of these groundwater samples fall Sodium or Potassium type. A few samples were under the Ca⁺ dominant type, remaining placed under Na⁺ and K⁺ dominant regions. In the anionic triangular field, 30% of the samples fall into the no-dominant type, and the rest 70 % of the samples are scattered into the chloride type and sulphate type region. In the year 2020, the groundwater samples fall in the cationic triangle in a similar pattern as in 2005; conversely, most of the samples shifted to chloride type in the anionic triangle. Hydrogeochemical facies in 2020 are Na-Cl followed by Ca-Mg-Cl. This indicated the seawater intrusion in the study area (Alfarrah et al., 2011; Shin et al., 2020).

182 Groundwater samples of no-dominant type were affected by seawater intrusion by
183 2020.

184 **3.3.2 The mechanism governing groundwater chemistry**



185

186

187

Fig. 4 Gibbs diagram in 2005 and 2020

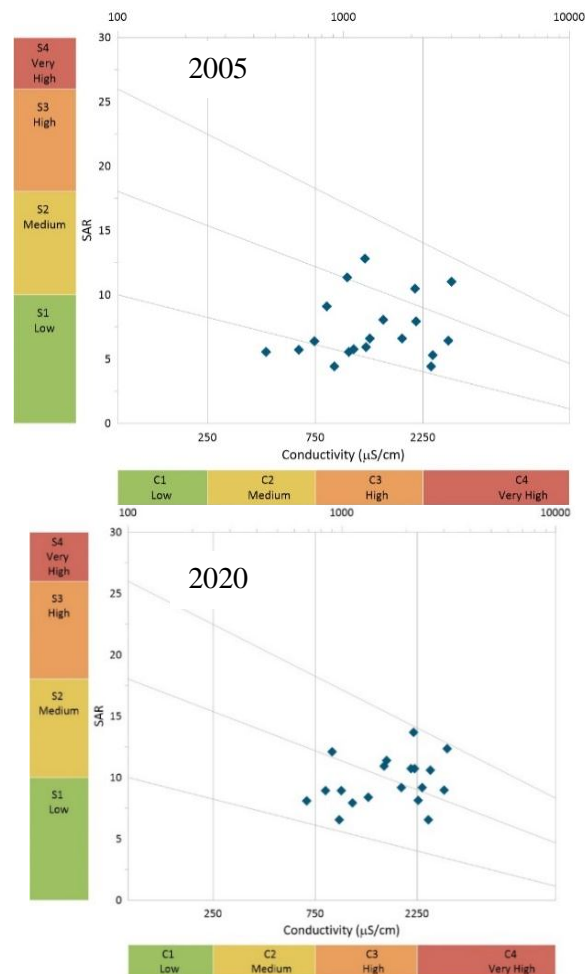
188 The diagram which expressed the mechanism that controls the chemical
189 composition of major dissolved salts in the groundwater was described using the
190 Gibbs Diagram. The chemical data of groundwater from unconfined and semiconfined
191 aquifers were plotted in the diagram (Fig. 4). Most of the aquifer samples, according
192 to Gibb's analysis, were found to be in the evaporation-dominating zone in both the
193 2005 and 2020 time periods, indicating that evaporation dominance is primarily
194 responsible for the groundwater chemistry in aquifers.

195 Most of the samples have large quantities of Cl^- , which suggests that Cl^- ions
 196 can come from a variety of sources. The distribution of Na^+ ions is concentrated
 197 largely at high proportions, suggesting that all Na^+ ions are formed from the same
 198 source or by the same geological process (Rao et al., 2017). In the aquifer, saltwater
 199 produces the ions Na^+ and Cl^- and the evaporation dominance on the diagrams
 200 shows seawater intrusion in the aquifer (Lanjwani et al., 2022; Sangadi et al., 2022).

201 3.4 Irrigation water quality

202 United States Salinity Laboratory diagram (USSSL diagram) is an approach to
 203 finding the groundwater quality for agriculture purposes, which was applied to realize
 204 the groundwater parameters (Richards, 1954). The results of the USSSL diagram (Fig.
 205 5) illustrate that most of the groundwater samples fall in the category of C3S2 (high
 206 salinity with medium sodium) followed by C4S2 (very high salinity with medium
 207 sodium). The electrical conductivity ranges from 1.87 to 4.2 dS/cm and SAR values
 208 range from 12 to 18. The result reveals that there is an occurrence of medium
 209 alkalinity and high to very high salinity hazards in the aquifer. The groundwater is not
 210 suitable for irrigation due to the presence of high salinity and little danger of
 211 exchangeable sodium (Ali & Ali, 2018).

212



213

214

Fig. 5 USSSL diagram in 2005 and 2020

215 According to the salinity hazard the majority of the samples were identified in
 216 the moderate salinity zone in 2005, but just a few samples were identified in this
 217 category in 2020. In contrast, the SAR values in 2005 and 2020 indicated that 55% of
 218 the samples had low to medium sodium adsorption ratios. Salinity hazard and SAR
 219 estimates were correlated, and the results showed that 65% of the samples were
 220 moderately suitable for agriculture in 2005 and 35% in 2020, whereas 35% of the
 221 samples were deemed unsuitable for agriculture in 2005 and 65% in 2020.

222 3.5 Spatial variability map of groundwater level in the unconfined 223 aquifer

224 One of the spatial interpolation techniques, ordinary kriging, is used to create
 225 the spatial variability maps of water table elevation and salinity that are shown in
 226 Figures 4.5 to 4.8. The maps can be used to comprehend the affected areas and rank
 227 them in terms of importance for incorporating various groundwater management
 228 plans into action. Three classes >2m, 2-4m, and >4m were used to define
 229 various groundwater level classes on the spatial maps. Based on the Central
 230 Pollution Control Board's classification, the area was divided into multiple EC classes
 231 (CPCB, 2018).

232 Pre-monsoon groundwater levels in both aquifers in 2005 ranged from -2 m to
 233 3.6 m, and post-monsoon levels ranged from -0.4 m to 5.4 m. In the unconfined and
 234 semiconfined aquifers, a reverse hydraulic gradient is present during both seasons.
 235 This reveals that seawater intrusion has occurred here. In the research region of the
 236 Vadakara stretch, the issue is contained at a 5 km distance from the sea (Northern
 237 coast). The unconfined aquifer's groundwater level fluctuated over this stretch
 238 between -2 m and 0.37 m in the pre-monsoon and -0.43 to 1.2 m in the post-
 239 monsoon. During the pre-monsoon, the area of the semiconfined aquifer's negative
 240 groundwater elevation was 6 km from the sea. In both aquifers, the area covered by
 241 different groundwater elevation classes was listed in Table 4.7. In the unconfined
 242 aquifer, the area with groundwater elevation of less than 2 m class in 2005 was
 243 24.4% in the pre-monsoon and 18.8% in the post-monsoon; by 2020, it was 28.7%
 244 and 21.5%, respectively. Similar patterns can be seen in the results from
 245 semiconfined aquifers. The recharge in both the aquifers during the monsoon may be
 246 responsible for the increase in groundwater level in the aquifer during post-monsoon.

247 Table 4.7 The delineated area under different water table elevation ranges

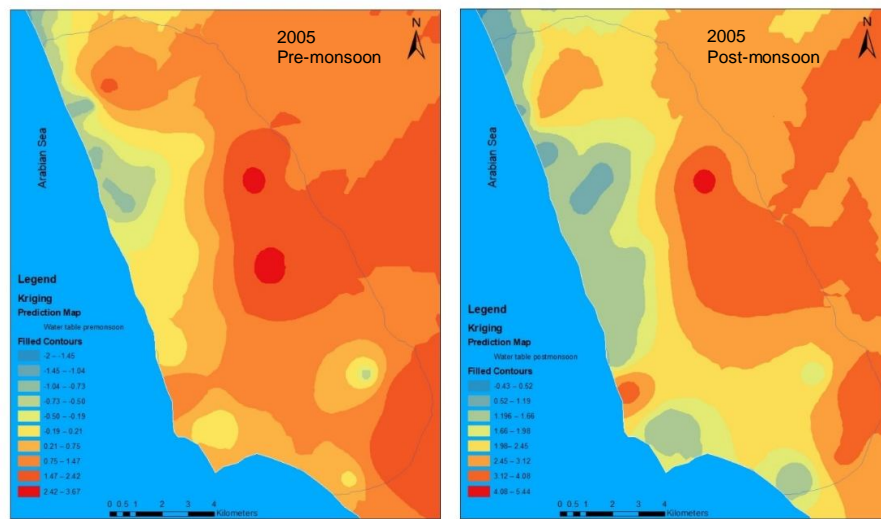
Aquifer	Water table elevation classes (m)	Area (%) 2005		Area (%) 2020	
		Pre-monsoon	Post-monsoon	Pre-monsoon	Post-monsoon
Unconfined	< 2	24.4	18.8	28.7	21.5
	2.0 - 4.0	39.3	51.6	39.1	44.9
	>4.0	36.3	29.6	32.2	33.6
Semiconfined	< 2	29.5	22.7	32.5	30.4
	2.0 - 4.0	38.4	48.8	37.9	44.7
	>4.0	32.1	28.5	29.6	24.9

248 Table 4.8 Delineated area under different Groundwater EC ranges

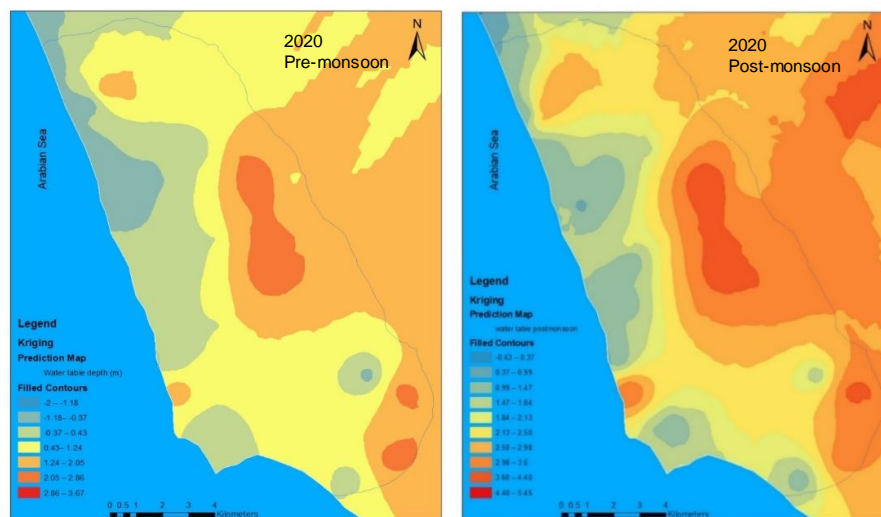
Aquifer	Groundwater	Area (%)	Area (%)
---------	-------------	----------	----------

	EC classes (dS/m)	2005		2020	
		Pre- monsoon	Post- monsoon	Pre- monsoon	Post- monsoon
Unconfined	< 0.75	27	39.5	23.1	31.6
	0.75-2.25	28.2	43.5	31.7	44.5
	2.25-4	26.8	17	20	23.9
	>4.0	18	0	25.2	0
Semiconfined	< 0.75	26.5	41.2	20.1	20.6
	0.75-2.25	25.3	39.6	21.7	45.5
	2.25-4	29.3	19.2	33.6	33.9
	>4.0	18.9	0	24.6	0

249



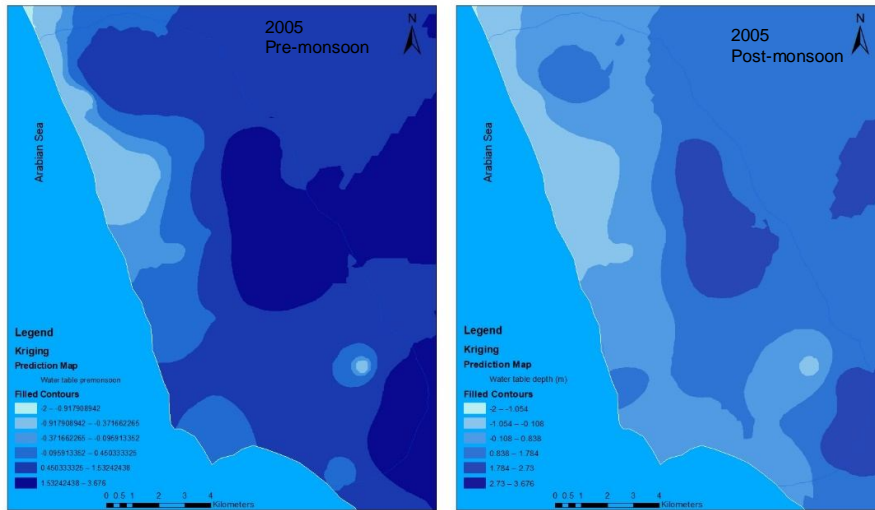
250



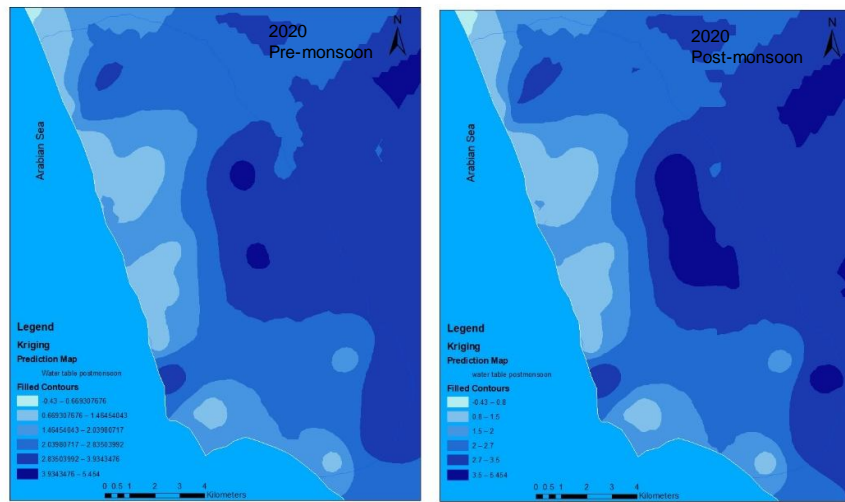
251

252

Fig. 4.5 Spatial variability map of the water table in the confined aquifer



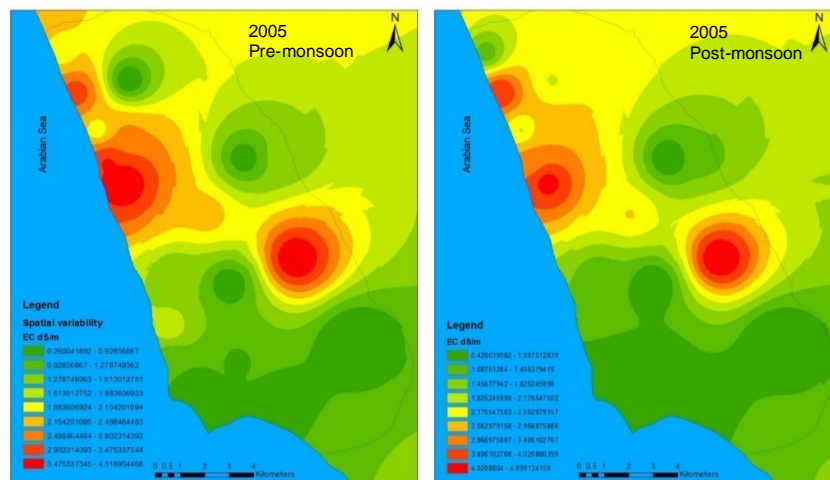
253



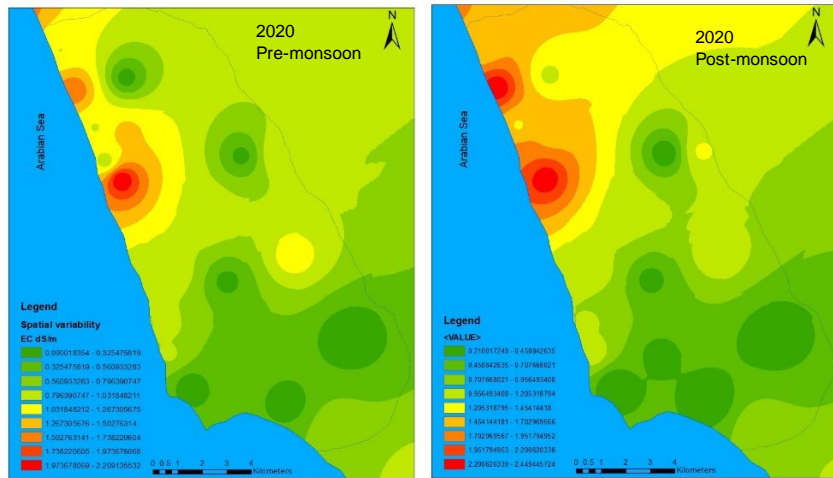
254

255

Fig. 4.6 Spatial variability map of the water table in the semi-confined aquifer

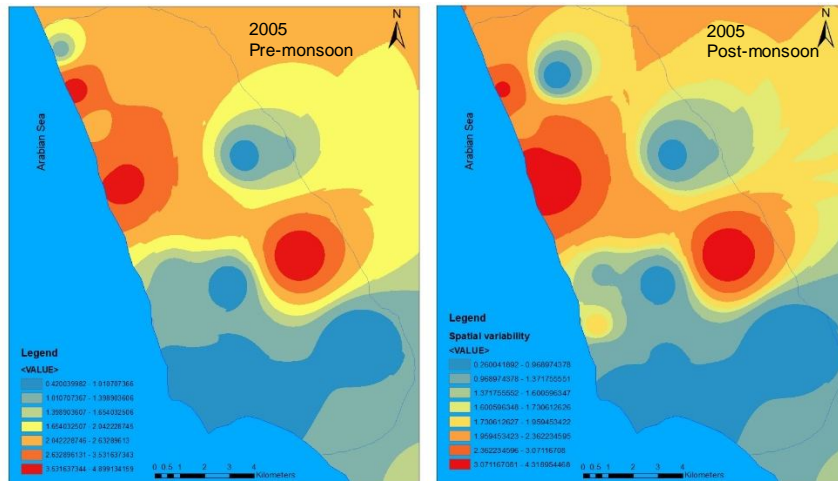


256

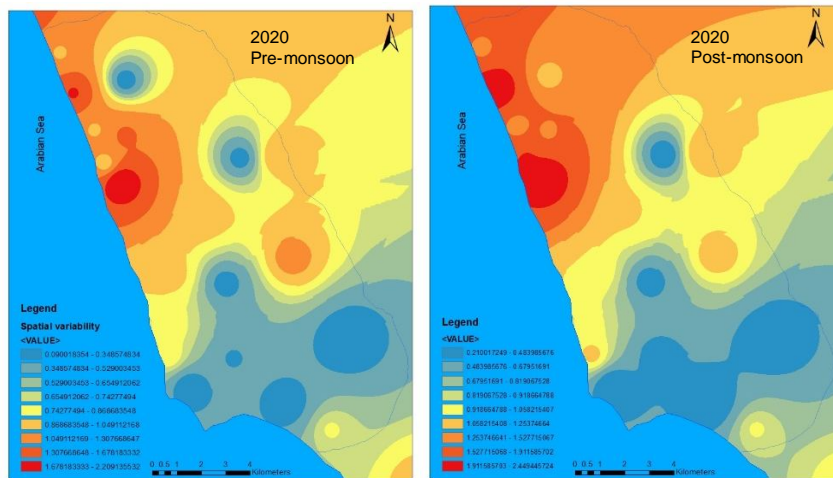


257
258

Fig. 4.7 Spatial variability map of the EC in the confined aquifer



259



260
261
262

Fig. 4.8 Spatial variability map of the EC in the semi-confined aquifer

263 The spatial variation of salinity (Table 4.8) reveals that, in 2005, pre-
264 monsoon, the EC of groundwater varies between 0.4 dS/m to 4.9dS/m in both the
265 aquifers and in post-monsoon it varies between -0.2 dS/m to 2.4dS/m. The study
266 area's northern coast shows higher EC than other regions. Along this stretch, the EC
267 variation in the unconfined aquifer was between -2.9 dS/m to 4.8 dS/m in pre-
268 monsoon and 1.5 dS/m to 2.2 dS/m in post-monsoon. Whereas in the semiconfined
269 aquifer it ranges from 2.1 dS/m m to 4.1 dS/m m and in post-monsoon 1.1 dS/m to
270 2.2 dS/m. The area under various groundwater EC classes in both the aquifers (Table
271 4.8) shows that, in 2005, the area under groundwater EC less than 2.25 dS/m class in
272 the unconfined aquifer was 55.2 % in pre-monsoon which increased to 83 % in post-
273 monsoon whereas it was estimated as 54.8% and 76.1 % respectively in 2020. The
274 area under groundwater EC greater than 4 dS/m class in the unconfined aquifer was
275 18 % in and 25.2 % in pre-monsoon in 2005 and 2020 respectively. However, in the
276 post-monsoon, there is no area existing in this class. The recharging in the
277 unconfined aquifer and recharging through the aquitard in the semiconfined aquifer
278 during the monsoon may be responsible for the post-monsoon increase in
279 groundwater quality. This might minimize the aquifer's reverse hydraulic gradient. The
280 percentage of land classified as "unfit for irrigation" increased by 7% over the course
281 of 15 years. The aquifer's declining groundwater level may increase the possibility of
282 salt and freshwater mixing, which could account for the reduction in water quality over
283 time.

284 4. Conclusion

285 The assessment of change in groundwater level and quality in the coastal
286 aquifer of Kozhikode district in Kerala was done based on physical and chemical
287 parameters, hydrogeochemical analysis, and spatial variations in groundwater levels
288 and salinity for the period 2005-2020. Reduction in groundwater level and
289 deterioration of groundwater quality premonsoon season in the study area were
290 identified even though there is an increase in annual rainfall over the period. The
291 change in Hydrochemical facies such as sulphates to chlorides in the anionic triangle
292 and the spatial distribution of groundwater samples in the evaporation dominance
293 zone in Gibbs plots reveal seawater intrusion into the wells. The irrigation water
294 quality of 45 % of the groundwater samples was changed to high to very high salinity
295 hazards in the aquifer during the 15 years. The groundwater level decreased during
296 pre-monsoon thereby the seawater intrusion into the freshwater aquifers reduced the
297 groundwater quality. However, the recharge of the aquifer from the monsoon
298 improves the condition in post-monsoon. The results may be used for planning
299 appropriate management strategies for managing the problem of seawater intrusion
300 during the premonsoon season in this region.

301 References

- 302 Alfarrak, N., Walraevens, K., Farrah, N. al, & Martens, K. (2011). Hydrochemistry of
303 the Upper Miocene-Pliocene-Quaternary aquifer complex of Jifarah Plain, NW-
304 Libya. *Geologica Belgica*, 14(3-4), 159-174.
- 305 Ali, S. A., & Ali, U. (2018). Hydrochemical characteristics and spatial analysis of
306 groundwater quality in parts of Bundelkhand Massif, India. *Applied Water*
307 *Science*, 8(1).
- 308 Arslan, H. (2012). Spatial and temporal mapping of groundwater salinity using
309 ordinary kriging and indicator kriging: The case of Bafra Plain, Turkey.
310 *Agricultural Water Management*, 113, 57-63.

- 311 CGWB. (2013). *Groundwater information booklet of Kozhikode district, Kerala state.*
- 312 Dash, C. J., Sarangi, A., & Singh, D. K. (2010). Spatial variability of groundwater
313 depth and quality parameters in the National Capital Territory of Delhi.
314 *Environmental Management*, 45, 640–650.
- 315 Gibbs, R. J. (1970). Mechanisms Controlling World Water Chemistry. *Science*,
316 170(3962), 1088–1090. <https://doi.org/10.1126/science.170.3962.1088>
- 317 Isaaks, E. H., & Srivastava, R. M. (1989). *An Introduction to Applied Geostatistics.*
318 Oxford University Press.
- 319 KSPCB. (2019). *Report On Restoration of Polluted River Stretches Draft Action Plan*
320 *Of River Kuttiyadi (Priority V).*
- 321 Lanjwani, M. F., Khuhawar, M. Y., Jahangir Khuhawar, T. M., Samtio, M. S., &
322 Memon, S. Q. (2021). Spatial variability and hydrogeochemical characterisation
323 of groundwaters in Larkana of Sindh, Pakistan. *Groundwater for Sustainable*
324 *Development*, 14. <https://doi.org/10.1016/j.gsd.2021.100632>
- 325 Lanjwani, M. F., Khuhawar, M. Y., Lanjwani, A. H., Khuahwar, T. M. J., Samtio, M. S.,
326 Rind, I. K., Soomro, W. A., Khokhar, L. A., & Channa, F. A. (2022). Spatial
327 variability and risk assessment of metals in groundwater of district Kamber-
328 Shahdadkot, Sindh, Pakistan. *Groundwater for Sustainable Development*,
329 100784. <https://doi.org/10.1016/j.gsd.2022.100784>
- 330 Michalopoulos, D., & Dimitriou, E. (2018). Assessment of Pollution Risk Mapping
331 Methods in an Eastern Mediterranean Catchment. *Journal of Ecological*
332 *Engineering*, 19, 55–68. <https://doi.org/10.12911/22998993/79646>
- 333 Nair, M. M. (1987). Coastal Geomorphology of Kerala. *Journal of The Geological*
334 *Society of India*, 29, 450–458.
- 335 Nazimuddin, M. (1993). *Coastal Hydrogeology of Kozhikode, Kerala Under the*
336 *Faculty Of Marine Sciences.*
- 337 Piper, A. M. (1944). A graphic procedure in the geochemical interpretation of water-
338 analyses. *Transactions, American Geophysical Union*, 25(6), 914.
339 <https://doi.org/10.1029/TR025i006p00914>
- 340 Rao, N. S., Vidyasagar, G., Surya Rao, P., & Bhanumurthy, P. (2017). Chemistry and
341 quality of groundwater in a coastal region of Andhra Pradesh, India. *Applied*
342 *Water Science*, 7(1), 285–294. <https://doi.org/10.1007/s13201-014-0244-0>
- 343 Richards, L. A. (1954). *Diagnosis and Improvement of Saline and Alkali Soils,*
344 *Agricultural Handbook* (Vol. 60). US Department of Agriculture.
- 345 Salaj, S. S., Ramesh, D., Suresh Babu, D. S., & Kaliraj, S. (2018). *Impacts of*
346 *urbanization on groundwater vulnerability along the Kozhikode coastal stretch,*
347 *Southwestern India using GIS based modified DRASTIC-U Model.*
348 www.jcsonline.co.nr
- 349 Sangadi, P., Kuppan, C., & Ravinathan, P. (2022). Effect of hydro-geochemical
350 processes and saltwater intrusion on groundwater quality and irrigational
351 suitability assessed by geo-statistical techniques in coastal region of eastern
352 Andhra Pradesh, India. *Marine Pollution Bulletin*, 175.
353 <https://doi.org/10.1016/j.marpolbul.2022.113390>
- 354 Sathiamoorthy, M., & Ganesan, M. (2018). *Hydro geochemical characterization of*
355 *surface and groundwater quality and assessing its suitability of drinking and*
356 *irrigational purposes in Veeranam tank area, Cuddalore district, Tamil Nadu,*
357 *India.* 23.

- 358 Shin, K., Koh, D. C., Jung, H., & Lee, J. (2020). The hydrogeochemical characteristics
359 of groundwater subjected to seawater intrusion in the Archipelago, Korea. *Water*
360 (*Switzerland*), 12(6). <https://doi.org/10.3390/W12061542>
- 361 Zhang, B., Zhao, D., Zhou, P., Qu, S., Liao, F., & Wang, G. (2020). Hydrochemical
362 characteristics of groundwater and dominant water-rock interactions in the
363 Delingha area, Qaidam Basin, Northwest China. *Water (Switzerland)*, 12(3).
364 <https://doi.org/10.3390/w12030836>